Electronic Supplementary Information for
The ACE2 receptor accelerates but is not biochemically required for SARS-CoV-2 membrane fusion.

Marcos Cervantes[1‡], Tobin Hess[1‡], Giorgio G. Morbioli[1‡†], Anjali Sengar[1], and Peter M. Kasson[1,2*]

1. Departments of Molecular Physiology and Biomedical Engineering, University of Virginia, Charlottesville VA 22908.
2. Science for Life Laboratory and Department of Molecular and Cellular Biology, Uppsala University, Uppsala SE 75123.

Supporting Methods

DNA-lipids.
DNA-lipids were synthesized as previously described[1] using DPPE azide and DBCO-functionalized DNA. DPPE-TAG TAT TCA ACA TTT CCG TGT CGA was added to liposomes, and DPPE-TTT TTT TTT TTT TTT TTT TTT TCG ACA CGG AAA TGT TGA ATA CTA was added to viral particles. The latter is complementary but includes a 24-mer poly-T spacer. These sequences correspond to sequences C and D previously reported for influenza tethering[1].

Liposomes.
Target liposomes were composed of 68.75 mol% POPC, 20% DOPE, 10 % cholesterol, 1% biotin-DPPE, 0.25 % Oregon Green-DHPE and extruded at 100 nm. Plasma membrane vesicles used for comparison were produced as previously reported[2]. Lipids (68.75 mol% POPC, 20% DOPE, 10 % chol, 1% biotin-DPPE, 0.25 % OG-DHPE) were mixed in chloroform and then dried under nitrogen to form a thin film. Films were stored under vacuum overnight, to ensure residual solvent removal, and then resuspended in 500 µL of reaction buffer (10 mM NaH_2PO_4, 90 mM sodium citrate, 150 mM NaCl, pH 7.4), and vortexed at low speeds for 5 min, until a milky suspension was formed. The suspension was subjected to 5 freeze-thaw cycles and then extruded 19 times through a 100 nm polycarbonate membrane, using a LiposoFast extruder (Avestin, Canada), to yield primarily large unilamellar vesicles. Lipid vesicles were stored in the dark, at 4 ºC, for no longer than 1 week. DNA functionalization of both viral particles and target liposomes was performed by adding DNA-lipids to either particles or liposomes at a concentration of 0.03 mol % lipid for liposomes and 0.2 µM for viral particles and incubating overnight at 4 ºC.

Pseudoviruses and virus-like particles.
Pseudovirus production was performed in HEK 293T cells as previously described[2, 3] using the following plasmids at ratios of 1: 0.22: 0.22: 0.22: 0.33: Luciferase-IRES-ZsGreen (BEI NR-52516) : HDM-Hgpm2 (BEI NR-52517) : pRC-CMV-Rev1b (BEI NR-52519) : HDM-tat1b (BEI NR-52518) : Spike- ALAYT (BEI NR-52515) following previously published protocols. These plasmids were gifts of Jesse Bloom. Omicron spike pseudotyping was performed using the plasmid pTwist-SARS-CoV-2 Δ18 B.1.1.529, a gift from Alejandro Balazs [4]. Pseudoviral supernatant was collected at 48 hours post transfection. Cellular debris was removed by centrifugation at 700 x g for 7 min at 4 ºC to remove cell debris followed by 0.45 µM filtration.
Virus-like particles were produced in 293T cells using plasmids encoding the M, N, E, and S proteins from SARS-CoV-2 in addition to a luciferase RNA carrying the SARS-CoV-2 PS9 sequence using previously published protocols [5]. Plasmids were a gift from Jennifer Doudna and are as follows: N (Addgene 177937); M and E (Addgene 177938); and S (D614G N501Y; Addgene 177939) along with a luciferase gene with SARS-CoV-2 packaging sequence PS9 into 293T cells (Addgene 177942.
Supernatants collected above were pelleted through a 25% sucrose cushion in HEPES-MES buffer (20 mm HEPES, 20 mm MES, 130 mm NaCl (pH 7.4)) at 140,000 x g for 2 h, 4 °C. Pellets were resuspended in HEPES-MES (20 mM HEPES, 20 mM MES, 130 mM NaCl, pH 7.4) buffer without sucrose to obtain a 100x concentration of the initial volume. Viral aliquots were stored at -80 °C and were thawed no more than once. Pseudoviruses and VLPs were handled under BSL-2 conditions with institutionally approved safety protocols.

Fluorescent labeling of pseudovirus particles and VLPs.
Pseudoviruses and VLPs were labeled with Texas Red-DHPE as follows. Briefly, 4 µL of TR-DHPE solution (0.75 mg/mL) were added to 240 µL of HEPES buffer. 200 µL of the staining solution were added to 50 µL of a 100X HIV pseudovirus or virus-like particle preparation (total viral protein concentration for HIV pseudovirus and virus-like particles were determined to be approximately 0.6 mg/mL and 2.9 mg/mL, respectively via a micro-BCA assay). After homogenization, the mixture was incubated in the dark on a rocker for 2 hours at room temperature. After the incubation, the solution was split into 2 centrifuge tubes, and 1.5 mL of HEPES buffer was added to each tube. Tubes were centrifuged for 1 hour at 4 ºC, at 20000 rcf. The supernatant was carefully discarded, and the pellets were resuspended in 25 µL of HEPES buffer in each tube.
Viral particles were then functionalized with DNA lipids as follows. DNA lipids were added to Texas-Red-labeled viral particles at a final concentration of 0.4 µM and incubated overnight, in the dark, at 4 ºC. Labeled pseudoviruses were stored in the dark at 4 ºC for no longer than 1 week.

Proteases and soluble ACE2.
Trypsin and TMPRSS2 were each prepared as follows. TPCK-treated trypsin (Sigma-Aldrich) was dissolved in reaction buffer (10 mM NaH_2PO_4, 90 mM sodium citrate, 150 mM NaCl, pH 7.4), and TMPRSS2 (Creative Biomart) was dissolved in DI water. Both were kept as frozen aliquots at -20 ºC at a concentration of 1,000 µg/mL, to be thawed, diluted, and warmed for immediate use for image acquisition. TMPRSS2 and trypsin activity were validated using a Boc-Gln-Ala-Arg-AMC fluorogenic substrate (Bachem).

ACE2 (MP Biomedicals) was expressed in a soluble dimeric form, residues 1-740. This enzyme was shipped in 8 M Urea, 20 mM Tris pH 8.0, 150 mM NaCl, 200 mM imidazole. Dialysis into 20 mM Tris pH 8.0, 150 mM NaCl, 200 mM imidazole was performed to remove urea using a dialysis slide with a 3.5 kDa cutoff (Thermo Scientific). The dialysis buffer was exchanged after 1.5 and 3 hours at room temperature; dialysis was continued overnight at 4 ºC. The concentration of dialyzed ACE2 was estimated at 812 µg/mL via absorbance at 280 nm. Aliquots were made and kept at -20 ºC to be thawed and diluted for immediate use.

Plasma membrane vesicles.
Plasma membrane vesicles were prepared as previously described[2]. Briefly, Calu-3 cells were cultured to 90% confluence in a 10-cm dish and then labeled with DiO membrane stain (Invitrogen) for 10 min. The plate was washed twice with PBS and then twice with GPMV buffer (10 mm HEPES, 150 mm NaCl, 2 mm $CaCl_2$, pH 7.4) to remove any unincorporated label. To induce vesiculation, the cells were incubated with 5 mL GPMV buffer to which 25 mM PFA and 2 mM DTT were added for two hours at 37 °C and 5% CO_2. The plates were placed on an orbital shaker for one hour at 37 ºC to detach the plasma membrane vesicles, and the supernatant was harvested. The supernatant was clarified via centrifugation at 100 x g for 10 min, and the precipitate was discarded. The resulting supernatant was concentrated via centrifugation at 20,000 x g for one hour at 4 ºC, and the pellet retained. The resulting vesicles were resuspended in 50 µL of GPMV buffer and incubated overnight with 1 µM biotin-PE in preparation for adhesion to flow cells.

Microfluidic flow cell preparation.
Glass coverslips (24 x 40 mm, No 1.5, VWR International) were washed in a solution of 7x detergent (MP Biomedicals) and DI water at a ratio of 1:7 under continuous stirring and heating until the solution appeared clear, approximately 15 minutes. Detergent was removed by rinsing in excess volumes of DI water and coverslips were then annealed in a kiln for 4 hours at 400 ºC. After cooling and several rinses with ultrapure water, coverslips were submerged in a bath sonicator for 5 minutes, rinsed with additional ultrapure water, sonicated again with absolute ethanol, and finally rinsed again with ultrapure water. Coverslips were then dried at 80 ºC for several hours and stored in an airtight tube.
Microfluidic flow-cell molds were made using soft lithography as summarized below. Briefly, Kapton polyimide tape (Ted Pella) was laid on a glass surface where multiple flow channels (1 mm x 13 mm x 70µm) were cut using a Cameo 4 cutter-plotter (Silhouette) and excess tape was removed. Polydimethylsiloxane (PDMS; Sylgard 184) was poured into molds after mixing at a ratio of 10:1 elastomer : curing agent, degassed under vacuum and cured at 60 ºC for 3 hours. After cooling, rectangular flow cells were sectioned out with influx/efflux holes made using a 2 mm biopsy punch.

Glass coverslips were plasma cleaned for 5 minutes (Harrick Plasma) and were then plasma bonded to PDMS flow cells after 1 minute plasma co-activation. Immediately afterwards, flow channels were flushed and coated with PLL-PEG : PLL-PEG-Biotin mixture (95% : 5%). After 30 minutes incubation at room temperature, channels were rinsed with 1 mL of ultrapure water and subsequently flushed with HEPES buffer (20 mM HEPES, 150 mM NaCl, pH 7.2). The channels were flushed with a 0.2 mg/mL solution of NeutrAvidin (Thermo Scientific), and the flow cell was incubated for 30 minutes at room temperature. After washing excess NeutrAvidin with 1 mL of HEPES buffer, channels were flushed with liposome reaction buffer (10 mM NaH_2PO_4, 90 mM sodium citrate, 150 mM NaCl, pH 7.4) and biotinylated liposomes functionalized with DNA-lipid conjugates were added, then left to incubate overnight at 4 ºC. Channels were washed to remove excess liposomes with 1 mL of reaction buffer before addition of viral agents.

Fusion experiments.
Biotinylated liposomes were bound to a PEGylated glass coverslip inside a microfluidic flow cell using PLL-PEG-biotin and neutravidin as previously described [6]. Texas-Red-labeled viral particles (either HIV-pseudovirus or virus-like particles) functionalized with DNA-lipid conjugates were diluted at an approximate ratio of 1:15 in 1.5% bovine serum albumin solution dissolved in liposome reaction buffer (10 mM NaH_2PO_4, 90 mM sodium citrate, 150 mM NaCl, pH 7.4) and immediately added to the flow cell channels. Flow cells were incubated at room temperature for 1 to 1.5 hours in the dark to allow for DNA-lipid conjugate binding and plastic reservoirs were affixed over the influx holes. Channels were rinsed with 1 mL of liposome reaction buffer to remove unbound viral particles. The fusion reaction was initiated by addition of soluble protease at pH 7.4 with or without soluble ACE2, and channels were imaged immediately at 37 ºC.

Immunofluorescence experiments
Display of spike protein on viral particles was verified by binding particles to liposomes using DNA-lipids as for fusion experiments, blocking with 1.5% BSA for 30 min, and then incubating with an anti-SARS-CoV-2 S monoclonal antibody (BEI Resources CR3022) at a 1:100 dilution in 1.5% BSA overnight at 4 ºC. The flow cell was then washed with HEPES buffer and then incubated with an Alexa 647-labeled goat anti-human secondary antibody (Invitrogen) at a 1:500 dilution for 90 minutes at room temperature. The flow cell was then washed again and imaged. A similar protocol was used for immunofluorescence staining of plasma membrane vesicles with the following modifications. Primary antibodies used were mouse anti-human ACE2 (Novus Biologicals NBP2-80035) and rabbit anti-human TMPRSS2 (Novus Biologicals 7B9W3), both at 1:200 dilution in 1.5% BSA. Washes were with 1 mL GPMV buffer, and secondary antibodies were Alexa 647 donkey anti-mouse (Invitrogen) and Alexa 568 goat anti-rabbit (Invitrogen), used at 1:100 and 1:5000 respectively. Secondary antibody incubation was for 60 minutes at room temperature.

Fluorescence microscopy and image analysis.
Video micrographs were acquired via epifluorescence microscopy using a 100x, 1.49 NA oil immersion objective and an Andor Zyla 4.2 sCMOS camera. Micrographs were recorded at 1 s intervals using a 150-ms exposure time using the MicroManager software[7]. The excitation light source was a Spectra X Light Engine (Lumencor), excitation/emission filters were 480/40 and 535/50 for Oregon Green and 560/40 and 630/75 for Texas Red. Images were acquired via a 100x oil immersion objective and a Zyla sCMOS 4.2 camera (Andor) at one-second intervals using a 150 ms exposure time. Micrographs were analyzed using previously reported single-virus detection and spot-tracking protocols,[8, 9] with an additional manual review stage for fusion events. Matlab code is available from https://github.com/kassonlab/ micrograph-spot-analysis. The number of fusion events compiled into each cumulative distribution function (CDF) is given in Table S1.

Supporting Figures and Tables

a. DNA

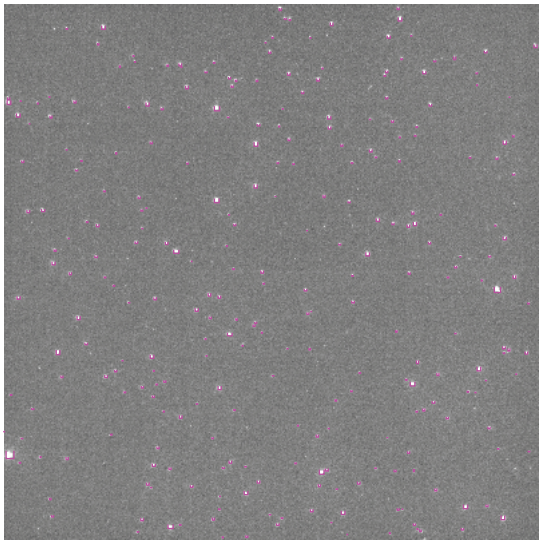

237 particles found

b. no DNA

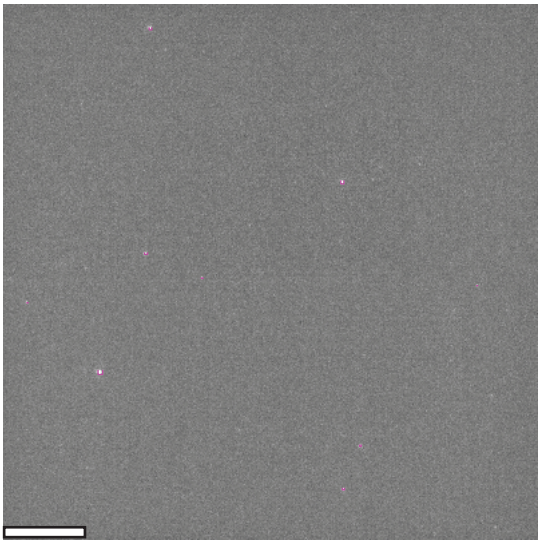

9 particles found

Figure S1. Low binding of labeled viral particles in the absence of DNA tethers. Micrographs show Texas-Red-labeled pseudovirus that was DNA-functionalized and allowed to bind to target liposomes either (a) containing complementary DNA-lipids or (b) without DNA-lipids. Unbound virus was washed away, and spots were counted, outlined in magenta. 237 particles bound when DNA-lipids were present, while only 9 particles bound without DNA-lipids. The latter likely represents nonspecific adsorption to the surface. Scale bar denotes 20 μm.

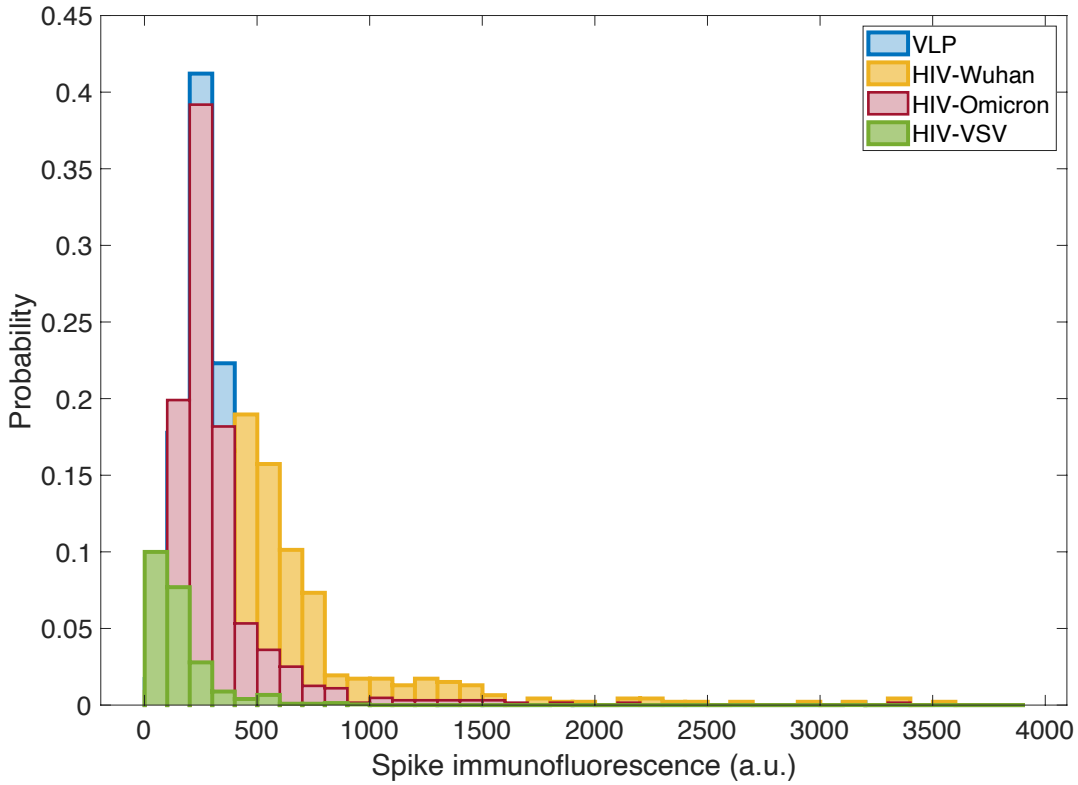

Figure S2. Single-particle immunofluorescence to detect SARS-CoV-2 spike protein. Pseudoviral or virus-like particles were produced, labeled, and then immobilized in a microfluidic flow cell following the same protocol as for fusion experiments. Immunostaining was then performed using an antibody that does not inhibit fusion (CR3022). Flow cells were then imaged, and fluorescent spots analyzed. VSV-G pseudoviruses on an HIV core were used as a negative control. 10 separate fields of view were imaged, and all were analyzed. Median background-subtracted fluorescence of spot total intensity was approximately 0 for VSV-G, 254 for Omicron pseudovirus, 268 for virus-like particles, and 512 for Wuhan pseudovirus. Median values of per-pixel averaged background-subtracted fluorescence values were 9 for VSV-G, 15 for Omicron pseudovirus, 16 for virus-like particles, and 30 for Wuhan pseudovirus. Some large bright spots were observed in the Wuhan samples that may have skewed the intensity distributions; these may represent viral aggregates.

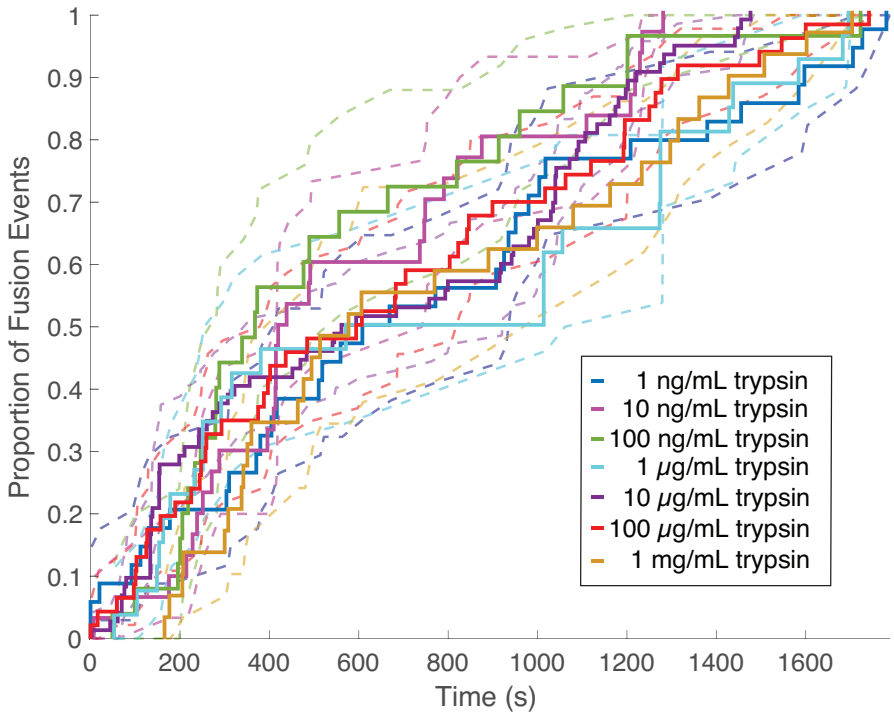

Figure S3. Cumulative distribution functions for fusion by DNA-tethered Wuhan pseudoviruses at different trypsin concentrations. Cumulative distribution functions are plotted for fusion experiments at ranges from 10 ng/mL to 1 mg/mL trypsin. This corresponds to panel c of Figure 3 but with confidence intervals generated via bootstrap resampling displayed. None of the distributions are significantly different from each other via 2-sample Kolmogorov-Smirnov tests, but all are significantly slower than when soluble ACE2 is added to 200 μg/mL trypsin (all p-values < 0.001 via 2-sample Kolmogorov-Smirnov tests).

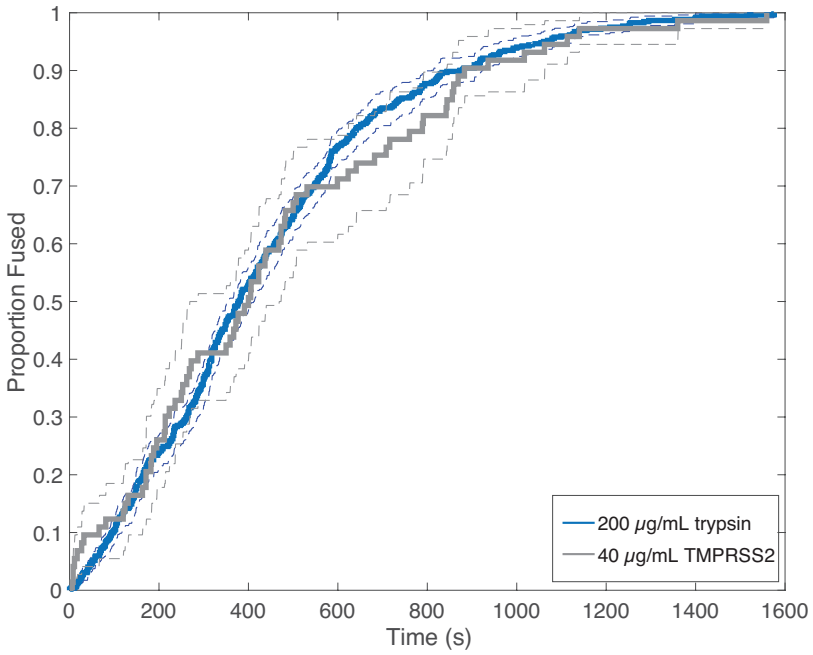

Figure S4. Comparison of fusion kinetics for virus-like particles activated with trypsin and TMPRSS2. The two distributions are statistically indistinguishable, with p > 0.73 via 2-sample Kolmogorov-Smirnov test.

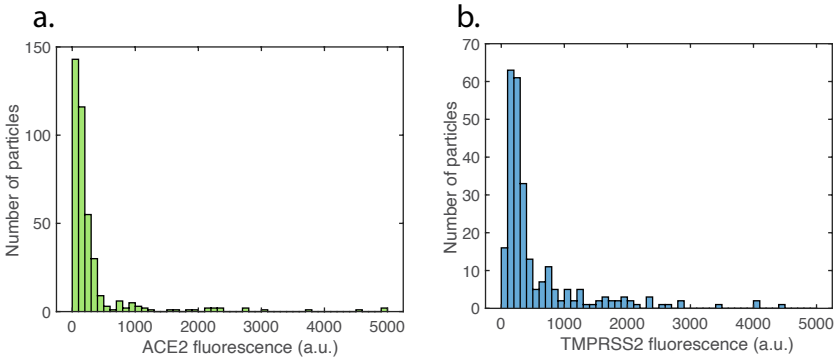

Figure S5. Immunostaining of Calu-3 plasma membrane vesicles. Plasma membrane vesicles were produced from Calu-3 cells and surface-immobilized in a microfluidic flow cell following the same protocol as for fusion experiments. Instead of virus, immunostaining was performed for ACE2 and TMPRSS2. Flow cells were then imaged, and fluorescent spots analyzed for membrane dye, ACE2 immunopositivity, and TMPRSS2 positivity. Histograms for the ACE2 and TMPRSS2-positive particles respectively are plotted in panels (a) and (b). 10 fields of view were imaged and analyzed. ACE2-positive particles were approximately 90% as abundant as overall PMV, and TMPRSS2-positive particles were approximately 60% as abundant.

a.

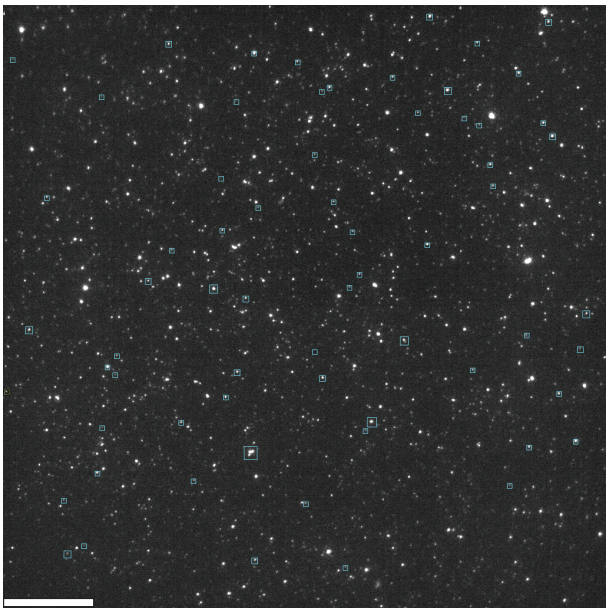

b.

Figure S6. Soluble ACE2 enhances SARS-CoV-2 spike-mediated fusion when added simultaneous to protease but reduces when added prior. Panels (a) and (b) show micrographs of Texas-Red-labeled pseudovirus tethered to liposomes after either addition of (a) 200 μg/mL trypsin simultaneous to soluble ACE2 or (b) soluble ACE2 added 15 minutes prior to trypsin. In panel (a), 65 dye dequenching events were observed, and the particles are outlined in cyan boxes. In panel (b), 8 dye dequenching events were observed. An additional experiment was performed where soluble ACE2 was added 70 minutes prior to trypsin, and only one dye dequenching event was observed. Scale bar denotes 20 μm.

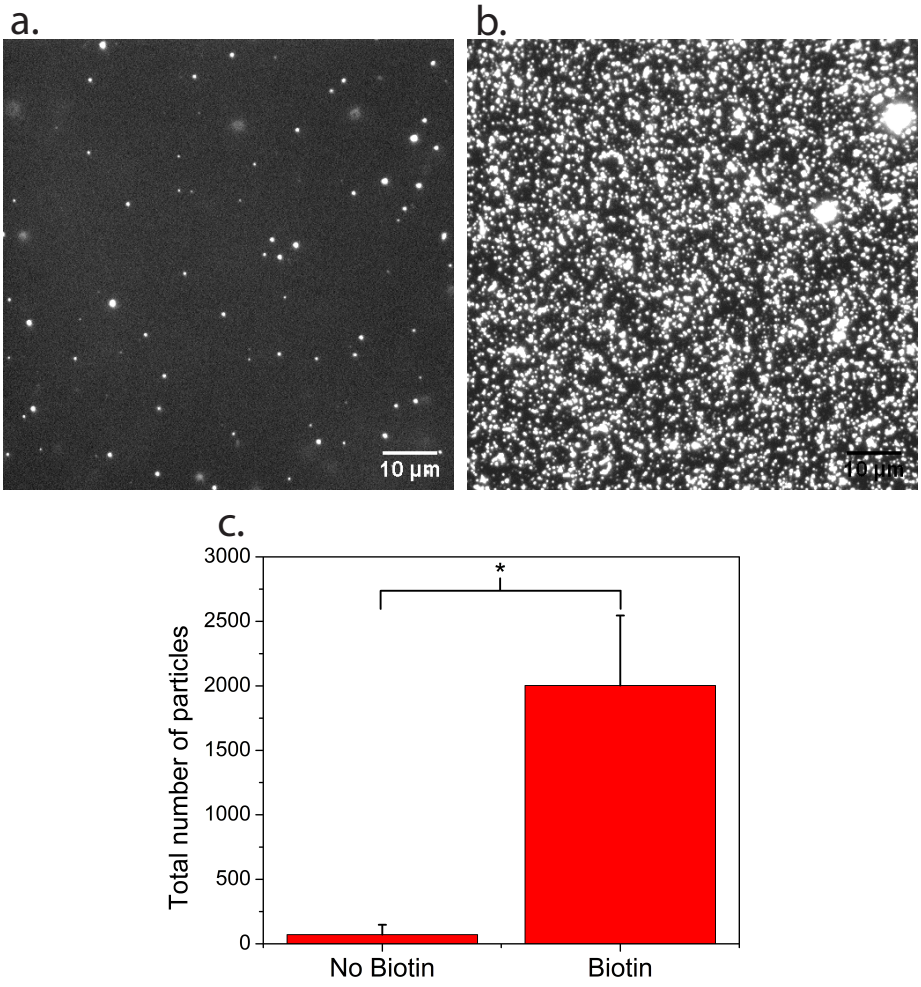

Figure S6. Low nonspecific binding in the absence of biotinylation. Micrographs in panels (a) and (b) show Oregon Green-labeled liposomes bound to the flow cell surface in (a) the absence of PLL-PEG-Biotin and (b) the presence of 2.5 % PLL-PEG-Biotin and neutravidin. Liposomes bonded to the flow cell channel surface via biotin-neutravidin-biotin binding. The number of bound liposomes is plotted in panel (c). In the presence of biotin, >20x more liposomes bound, $p < 0.05$ via t-test. Scale bars in the micrographs denote 10 µm. Micrographs were recorded using an Andor iXon Ultra 897 EMCCD camera.

Pseudovirus:	Protease:	Co-factor:	# of lipid mixing events:	# of lipid mixing events per FOV	Lipid-mixing efficiency
Wuhan / HIV pseudovirus	1 ng/mL trypsin		34	17	5.0%
Wuhan / HIV pseudovirus	10 ng/mL trypsin		25	25	4.1%

Wuhan / HIV pseudovirus	100 ng/mL trypsin		30	30	2.7%
Wuhan / HIV pseudovirus	1 µg/mL trypsin		26	26	11.6%
Wuhan / HIV pseudovirus	10 µg/mL trypsin		72	36	3.0%
Wuhan / HIV pseudovirus	100 µg/mL trypsin		46	46	5.3%
Wuhan / HIV pseudovirus	200 µg/mL trypsin		320	106	13.8%
Wuhan / HIV pseudovirus	500 µg/mL trypsin		99	50	17.4%
Wuhan / HIV pseudovirus	1000 µg/mL trypsin		146	29	8.7%
Wuhan / HIV pseudovirus	200 µg/mL trypsin	ACE2	65	65	7.1%
Wuhan / HIV pseudovirus	100 µg/mL trypsin	ACE2, 5 min	45	22.5	3.4%
Wuhan / HIV pseudovirus	100 µg/mL trypsin	ACE2, 10 min	50	50	3.6%
Wuhan / HIV pseudovirus	100 µg/mL trypsin	ACE2, 15 min	20	20	2.5%
Wuhan / HIV pseudovirus	100 µg/mL trypsin	ACE2, 20 min	28	28	5.5%
Wuhan / HIV pseudovirus	100 µg/mL trypsin	120 µg/mL ACE2	42	21	2.8%
Wuhan / HIV pseudovirus	100 µg/mL trypsin	ACE2	21	21	2.9%
Omicron / HIV pseudovirus	200 µg/mL trypsin		30	3	1.8%
Omicron / HIV pseudovirus	500 µg/mL trypsin		78	18	5.7%
Omicron / HIV pseudovirus	1000 µg/mL trypsin		170	41	11.9%
Omicron / HIV pseudovirus	200 µg/mL trypsin	ACE2	207	14.8	9.0%
D614G, N501Y / VLP	200 µg/mL trypsin		522	261	14.7%
D614G, N501Y / VLP	40 µg/mL TMPRSS2		73	73	5.7%
Wuhan / HIV pseudovirus		PMV containing ACE2 and TMPRSS2	24	24	13.0%

Table S1. Numbers of fusion events observed for each condition reported. We note that fusion efficiency values are more variable across experiments and are best compared

using parallel experimental design (one flow cell channel per condition and comparing results). Kinetics are quite robust across experiments.

All parameters variable:

	N	τ	Lag (s)	R^2
Wuhan	1.9	337	0.0053	0.995
Omicron	2.3	259	1.05e-04	0.989
Wuhan + ACE2	0.81	327	4.46	0.988
Omicron + ACE2	2.0	205	6.76	0.996

Fixed N, variable tau:

	N	τ (s)	Lag (s)	R^2
Wuhan	2.0	300	0.0001	0.992
Omicron	2.0	295	0.0001	0.989
Wuhan + ACE2	2.0	113	0.0001	0.926
Omicron + ACE2	2.0	203	0.0001	0.992

Fixed tau, variable N:

	N	τ (s)	Lag (s)	R^2
Wuhan	2.5	242	4.01	0.983
Omicron	2.4	242	4.01	0.987
Wuhan + ACE2	1.0	242	4.01	0.989
Omicron + ACE2	1.8	242	4.01	0.992

Table S2. Gamma fit parameters corresponding to Figure 5. Lipid mixing cumulative distribution functions were fit to a gamma function as indicated in the text with an additional time phase-shift parameter denoted "lag" to test for the presence of any substantial lag phase (see ref [10]). All fitted values of this parameter were < 7 seconds, and most approached zero.

References

1. A. Sengar, M. Cervantes and P. M. Kasson, *Biophysical Journal*, 2022, DOI: 10.1016/j.bpj.2022.10.026, 2022.2008.2003.502654.
2. A. Sengar, S. T. Bondalapati and P. M. Kasson, *bioRxiv*, 2021, DOI: 10.1101/2021.05.04.442634, 2021.2005.2004.442634.
3. K. H. D. Crawford, R. Eguia, A. S. Dingens, A. N. Loes, K. D. Malone, C. R. Wolf, H. Y. Chu, M. A. Tortorici, D. Veesler, M. Murphy, D. Pettie, N. P. King, A. B. Balazs and J. D. Bloom, *Viruses*, 2020, **12**.
4. W. F. Garcia-Beltran, K. J. St. Denis, A. Hoelzemer, E. C. Lam, A. D. Nitido, M. L. Sheehan, C. Berrios, O. Ofoman, C. C. Chang, B. M. Hauser, J. Feldman, A. L. Roederer, D. J.

Gregory, M. C. Poznansky, A. G. Schmidt, A. J. Iafrate, V. Naranbhai and A. B. Balazs, *Cell*, 2022, **185**, 457-466.e454.
5. A. M. Syed, T. Y. Taha, T. Tabata, I. P. Chen, A. Ciling, M. M. Khalid, B. Sreekumar, P.-Y. Chen, J. M. Hayashi, K. M. Soczek, M. Ott and J. Doudna, *Science*, 2021, **374**, 1626-1632.
6. A. M. Villamil Giraldo and P. Kasson, *Journal of Physical Chemistry Letters*, 2020, **11**, 7190-7196.
7. A. D. Edelstein, M. A. Tsuchida, N. Amodaj, H. Pinkard, R. D. Vale and N. Stuurman, *J Biol Methods*, 2014, **1**.
8. R. J. Rawle, S. G. Boxer and P. M. Kasson, *Biophys J*, 2016, **111**, 123-131.
9. R. J. Rawle, A. M. Villamil Giraldo, S. G. Boxer and P. M. Kasson, *Biophys J*, 2019, **117**, 445-452.
10. R. J. Rawle, E. R. Webster, M. Jelen, P. M. Kasson and S. G. Boxer, *ACS Central Science*, 2018.